

Update of the $H \rightarrow WW^{(*)} \rightarrow e\nu\mu\nu$ analysis with 13.0 fb^{-1} of $\sqrt{s} = 8 \text{ TeV}$ data collected with the ATLAS detector

Keisuke Yoshihara^{1,a}, On behalf of ATLAS Collaboration.

¹The University of Tokyo, 7-3-1 Hongo, Bunkyo ward, Tokyo, Japan

Abstract. An update of the $H \rightarrow WW^{(*)} \rightarrow e\nu\mu\nu$ analysis has been performed with the ATLAS detector at the LHC. The analysis focuses on the mass region around 125 GeV where a discovery of a new neutral boson was made in 2012.

1 Introduction

The ATLAS [1] and CMS [2] collaborations have recently reported on significant excesses of events in the searches for the SM Higgs boson [3, 4]. These searches combine multiple final states and use LHC pp collision data corresponding to 5 fb^{-1} of integrated luminosity at $\sqrt{s} = 7 \text{ TeV}$ and 6 fb^{-1} at $\sqrt{s} = 8 \text{ TeV}$. The ATLAS collaboration reported a new neutral boson with a measured mass of $m_H = 126.0 \pm 0.4 \text{ (stat)} \pm 0.4 \text{ (syst)} \text{ GeV}$ with a local significance of 5.9 standard deviations. The CMS collaboration reported a similar observation, with an excess of 5.0 standard deviations at $m_H = 125.3 \pm 0.4 \text{ (stat)} \pm 0.5 \text{ (syst)} \text{ GeV}$.

Now that the existence of a new particle has been established by these searches, the focus of the experimental work turns to the consistency of the observed particle with the predictions of the Standard Model. The $H \rightarrow WW^{(*)} \rightarrow \ell\nu\ell\nu$ channel (with $\ell = e, \mu$) provides important information on both the overall production rate and the coupling to W bosons.

The analysis presented here is predominantly sensitive to Higgs boson production via the dominant gluon-gluon fusion (ggF) process. The hypothesis of a SM Higgs boson with $m_H = 125 \text{ GeV}$, compatible with the observed excess, is used to characterise the signal. As with the earlier 2012 analysis, only results in the $e\nu\mu\nu$ final state, which provide the large majority of the sensitivity of the analysis, are presented based on the conference note [5].

2 Event Selection

$H \rightarrow WW^{(*)} \rightarrow \ell\nu\ell\nu$ candidates (with $\ell = e, \mu$) are pre-selected by requiring exactly two oppositely charged isolated leptons of different flavours, with p_T thresholds of 25 GeV and 15 GeV for the leading and sub-leading lepton, respectively. The dilepton invariant mass is required to be greater than 10 GeV. Drell-Yan and multijet events are suppressed by requiring large E_T^{miss} . The E_T^{miss} is the

magnitude of $\mathbf{p}_T^{\text{miss}}$, the opposite of the vector sum of the transverse energy of the reconstructed objects, including muons, electrons, photons, jets, and clusters of calorimeter cells not associated with these objects. After the lepton isolation and E_T^{miss} requirements, the multijet background is negligible and the Drell-Yan background is much reduced. Any multijet background present at this stage is included in the W +jets background estimate.

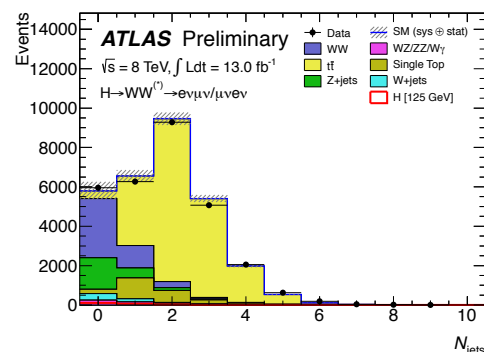


Figure 1. Multiplicity of jets for events satisfying the pre-selection criteria [5] described in the text. The hashed area indicates the total uncertainty on the background prediction. The WW and top backgrounds are scaled to use the normalization derived from the corresponding control regions described in the text.

The background rate and composition depend significantly on the jet multiplicity, as does the signal production mechanism. Without accompanying jets, the signal originates almost entirely from the ggF process and the background is dominated by WW events. In contrast, when produced in association with two or more jets, the signal contains a much larger contribution from the VBF process and the background is dominated by $t\bar{t}$ production. In this note only the zero and one jet analyses, which are most sensitive to a ggF signal, are presented. To further max-

^ae-mail: Keisuke.Yoshihara@cern.ch

imise the sensitivity, different selection criteria for events with zero and one accompanying jets passing the jet requirements, are applied to the pre-selected sample. Due to spin correlations in the $WW^{(*)}$ system arising from the spin-0 nature of the SM Higgs boson and the V-A structure of the W boson decay, the charged leptons tend to emerge from the interaction pointing in the same direction. This kinematic feature is exploited for both jet multiplicities by requiring that the dilepton invariant mass, $m_{\ell\ell}$, be less than 50 GeV and that the azimuthal angular difference between the leptons, $\Delta\phi_{\ell\ell}$, be less than 1.8 radians. In the $H+0$ -jet channel, the magnitude $p_T^{\ell\ell}$ of the transverse momentum of the dilepton system is required to be greater than 30 GeV. This improves the rejection of the Drell-Yan background. In the $H+1$ -jet channel, backgrounds from top quark decays are suppressed by rejecting events containing a jet identified as being consistent with originating from the decay of a b or c quark (b -tagged jet), using a b -tagging algorithm based on a neural network. A transverse mass variable, m_T , is used in this analysis to test for the presence of a signal for both jet multiplicities. This variable is defined as:

$$m_T = \sqrt{(E_T^{\ell\ell} + E_T^{\text{miss}})^2 - |\mathbf{p}_T^{\ell\ell} + \mathbf{p}_T^{\text{miss}}|^2},$$

where $E_T^{\ell\ell} = \sqrt{|\mathbf{p}_T^{\ell\ell}|^2 + m_{\ell\ell}^2}$. The statistical analysis uses a fit to the m_T shape in the signal region data after the $\Delta\phi_{\ell\ell}$ requirement.

3 Background estimate

The leading backgrounds from SM processes are WW and top quark production. The contributions from WW and top quark processes, as well as the smaller but significant $Z/\gamma^* \rightarrow \tau\tau$ background, are normalized to observed rates in data in control regions dominated by the relevant background source. The W +jets background is fully estimated from data. The shapes and normalization of backgrounds from diboson processes other than WW are estimated using simulation. The simulation predictions for these backgrounds are however cross-checked, together with the W +jets data-driven estimation, in a selection in which the two lepton candidates are required to have the same charge. This “validation region” is distinguished from the “control regions”, which are used to directly normalize the corresponding backgrounds. The control and validation regions are defined by selections similar to those used in the signal region but with some criteria reversed or modified to obtain signal-depleted samples enriched in a particular background. The WW background in both the $H+0$ -jet and $H+1$ -jet analyses and the top background in the $H+1$ -jet analysis are normalized to the data yields in the corresponding control regions, after subtracting contributions from processes other than the targeted one. The resulting estimated event yield for that process is extrapolated from the control region to the signal region using the ratio of event yields in the simulation. Using only a ratio of event yields from the simulation rather than

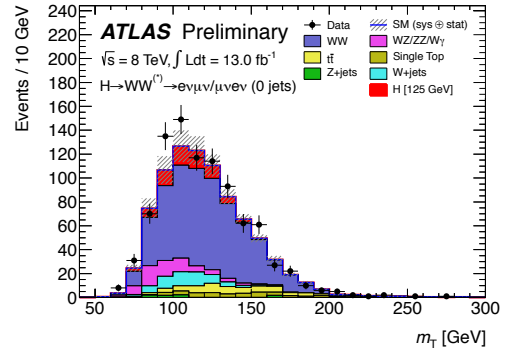


Figure 2. m_T distribution in the signal region [5] in $H+0$ -jet analysis. The lepton flavours are combined. The expected signal for a SM Higgs boson with $m_H = 125$ GeV is added on top of the estimated total background. The W +jets background is estimated from data and WW , top and $Z/\gamma^* \rightarrow \tau\tau$ backgrounds are scaled to use the normalization derived from the corresponding control regions. The hashed area indicates the total uncertainty on the background prediction.

Table 1. Dominant contributions to the relative uncertainty on the measured signal strength for $m_H = 125$ GeV [5]. The total relative uncertainty is also given.

Source	+ (%)	- (%)
Statistical uncertainty	+23	-22
Signal yield ($\sigma \cdot \mathcal{B}$)	+14	-9
Signal acceptance	+9	-6
WW normalization, theory	+20	-20
Other backgrounds, theory	+9	-9
W +jets fake rate	+11	-12
Experimental + bkg subtraction	+14	-11
MC statistics	+8	-8
Total uncertainty	+41	-38

the absolute prediction reduces the sensitivity of the background predictions to the systematic uncertainties, which are detailed in the next section. The correlations introduced among the backgrounds by the presence of other processes in the control regions are fully incorporated in the profile likelihood used to test the background-only hypothesis and extract the signal strength.

4 Systematic uncertainties

The systematic uncertainties can be divided into two categories: experimental uncertainties such as those on the jet energy scale and the b -jet tagging efficiency, and theoretical uncertainties such as the estimation of the effect of higher-order terms through variations of the QCD scale inputs to Monte Carlo calculations. Some of them are correlated between the signal and background predictions, so the impact of each uncertainty is calculated by varying the parameter in question and coherently recalculating the signal and backgrounds. The systematics on the background are dominated by both experimental and theoretical ones, while the signal cross section uncertainty is dominated by theoretical ones. The details are shown in the next section.

5 Results

The m_T distribution of events satisfying all of the criteria up to and including the $\Delta\phi_{\ell\ell}$ requirement is fit using the binned likelihood $\mathcal{L}(\mu, \theta)$, which is constructed as the product of Poisson probability terms in each lepton flavour channel, with the $H + 0$ -jet ($H + 1$ -jet) signal regions subdivided into five (three) m_T bins. A signal strength parameter μ multiplies the expected Standard Model Higgs boson production signal in each bin. Signal and background predictions depend on systematic uncertainties that are parametrized by nuisance parameters θ , which in turn are constrained using Gaussian functions. The expected signal and background event counts in each bin are functions of θ .

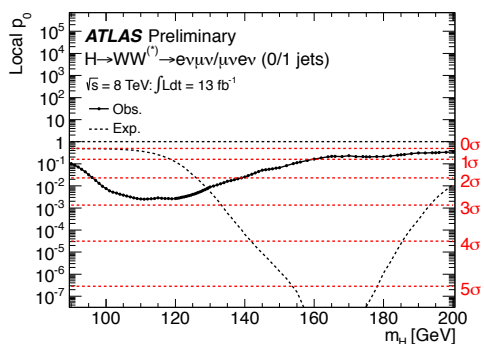


Figure 3. Observed probability for the background-only scenario as a function of m_H [5]. The dashed line shows the corresponding expectation for the signal+background hypothesis at the given value of m_H .

The parametrization is chosen such that the rates in each channel are log-normally distributed for a normally distributed θ . A test statistic q_μ is constructed using the profile likelihood: $q_\mu = -2 \ln(\mathcal{L}(\mu, \hat{\theta}_\mu) / \mathcal{L}(\hat{\mu}, \hat{\theta}))$, where $\hat{\mu}$ and $\hat{\theta}$ are the parameters that maximize the likelihood (with the constraint $0 \leq \hat{\mu} \leq \mu$), and $\hat{\theta}_\mu$ are the nuisance parameter values that maximize the likelihood for a given μ . Figure 3 and 4 show the expected and observed p_0 value and the fitted signal strength μ for the combined analyses. An excess of events is observed over the expected background, reflected by the low observed p_0 and a fitted μ which deviates from zero. Due to the limited mass resolution in the $H \rightarrow WW^{(*)} \rightarrow \ell\nu\ell\nu$ channel, the p_0 distribution is rather flat around $m_H = 125$ GeV. The observed value of p_0 at $m_H = 125$ GeV is 4×10^{-3} , corresponding to 2.6 standard deviations.

For p_0 and signal strength, the systematic uncertainty includes a small but non-negligible contribution from the statistical uncertainty on analysis inputs derived from simulation. The expected precision is improved relative to the previous analysis, primarily due to the increase in integrated luminosity. The precision of the analysis is now limited by the systematic uncertainties.

After dividing out the predicted Standard Model cross section and removing the associated uncertainties on the

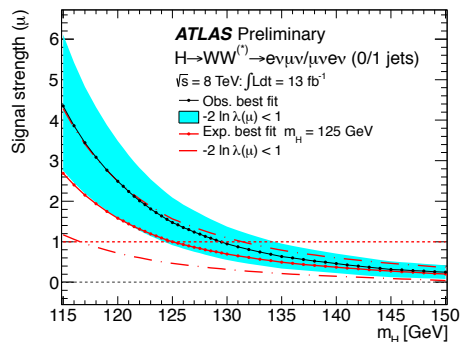


Figure 4. Fitted signal strength parameter (μ) as a function of m_H for the low mass range [5]. The expected result for an injected signal with $m_H = 125$ GeV (continuous red line) is included for comparison. The uncertainty on μ corresponds to the two crossings at $-2 \ln \lambda(\mu) = 1$.

signal yield, the measured product of the measured cross section times branching ratio at $m_H = 125$ GeV is

$$\begin{aligned} & \sigma(pp \rightarrow H) \cdot \mathcal{B}(H \rightarrow WW)_{m_H=125 \text{ GeV}} \\ &= 7.0^{+1.7}_{-1.6} (\text{stat})^{+1.7}_{-1.6} (\text{syst theor})^{+1.3}_{-1.3} (\text{syst exp}) \pm 0.3 (\text{lumi}) \text{ pb} \end{aligned}$$

6 Conclusion

An analysis of the $H \rightarrow WW^{(*)} \rightarrow \ell\nu\ell\nu$ channel has been performed using 13.0 fb^{-1} data from the LHC at $\sqrt{s} = 8$ TeV recorded in 2012 with the ATLAS detector. An excess of events over the expected background is observed for $m_H \lesssim 150$ GeV. These observations are consistent with the decay of the newly discovered boson [3] into a pair of W bosons. The addition of 7.2 fb^{-1} of data to the 5.8 fb^{-1} results presented in Ref. [5], improves the sensitivity of the signal strength measurement.

References

- [1] ATLAS Collaboration, 2008 JINST 3 S08003.
- [2] CMS Collaboration, 2008 JINST 3 S08004.
- [3] ATLAS Collaboration, *Observation of a new particle in the search for the Standard Model Higgs boson with the ATLAS detector at the LHC*, Phys. Lett. B **716** (2012) 1–29. 39 p, <http://arxiv.org/abs/1207.7214> arXiv:1207.7214 [hep-ph].
- [4] CMS Collaboration, *Observation of a new boson at a mass of 125 GeV with the CMS experiment at the LHC*, Phys. Lett. B **716** (2012) 30–61. 59 p, <http://arxiv.org/abs/1207.7235> arXiv:1207.7235 [hep-ph].
- [5] ATLAS Collaboration, *Update of the $H \rightarrow WW^{(*)} \rightarrow \ell\nu\ell\nu$ Analysis with the ATLAS Detector*, ATLAS-CONF-2012-158, 2012. <https://cdsweb.cern.ch/record/1493601>